Stair Blue Noise Sampling

Bhavya Kailkhura[†‡], Jayaraman J. Thiagarajan[‡], Peer-Timo Bremer[‡] and Pramod K. Varshney[†]
[†]Syracuse University, [‡]Lawrence Livermore National Laboratory

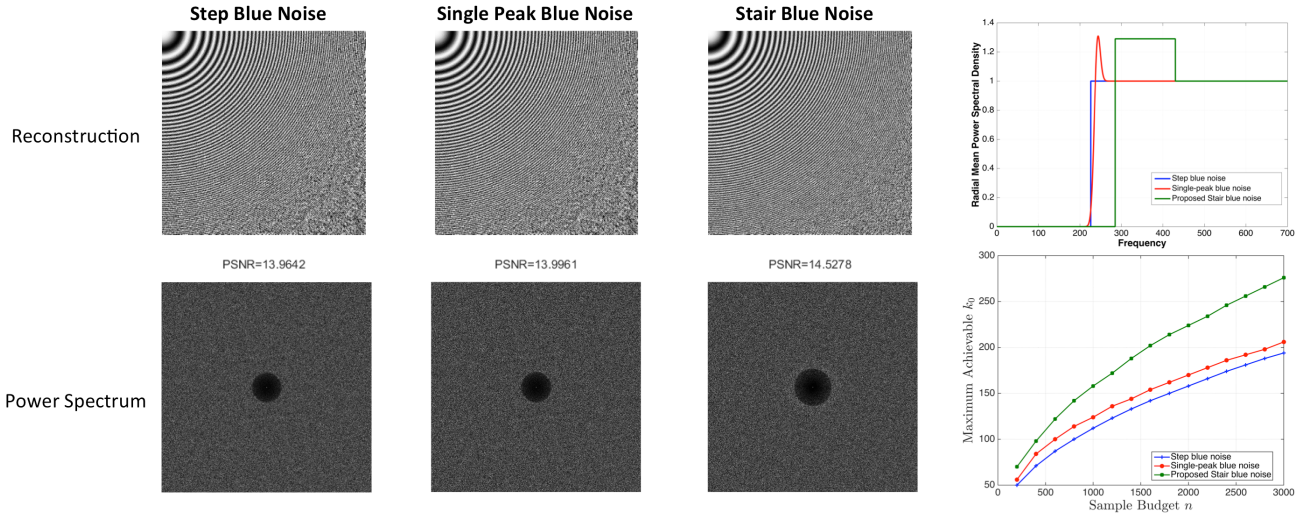

Figure 1: *Comparison of different blue noise distributions - reconstructions of the zone-plate function using* 4096 *samples. In contrast to the Single Peak blue noise distribution considered in [Heck et al. 2013], the proposed Stair blue noise achieves a significantly larger zero-region in the low frequencies without introducing discernible mid-frequency aliasing. A Single Peak blue noise distribution with its peak power in the radial mean power spectrum constrained to that of the Stair blue noise is only marginally better than Step blue noise. The improvement in the size of the maximum achievable, alias-free zero region is observed for all sample sizes. For instance, the zero region achieved by* 2000 *samples of Step and Single Peak blue noise can be achieved by only* 1000 *Stair blue noise samples.*

Abstract

A common solution to reducing visible aliasing artifacts in image reconstruction is to employ sampling patterns with a blue noise power spectrum. These sampling patterns can prevent discernible artifacts by replacing them with incoherent noise. Here, we propose a new family of blue noise distributions, *Stair blue noise*, which is mathematically tractable and enables parameter optimization to obtain the optimal sampling distribution. Furthermore, for a given sample budget, the proposed blue noise distribution achieves a significantly larger alias-free low-frequency region compared to existing approaches, without introducing visible artifacts in the mid-frequencies. We also develop a new sample synthesis algorithm that benefits from the use of an unbiased spatial statistics estimator and efficient optimization strategies.

Keywords: sampling, blue noise, anti-aliasing, pair correlation function

Concepts: •**Computing methodologies** → **Rendering; Antialiasing;** *Image processing;*

SA '16 Technical Papers,, December 05-08, 2016, Macao
ISBN: 978-1-4503-4514-9/16/12
DOI: http://dx.doi.org/10.1145/2980179.2982435

ACM Reference Format
Kailkhura, B., Thiagarajan, J., Bremer, P., Varshney, P. 2016. Stair Blue Noise Sampling. ACM Trans. Graph. 35, 6, Article 248 (November 2016), 10 pages. DOI = 10.1145/2980179.2982435
http://doi.acm.org/10.1145/2980179.2982435.

1 Introduction

Sampling images for subsequent reconstruction is one of the fundamental problems in computer graphics. The challenge is that images are rarely band-limited and thus some aliasing, i.e. sampling artifacts, cannot be avoided. However, it is well known that aliasing can be made less visible by introducing randomness in the sampling patterns. The optimal solution in this respect are *blue noise* type patterns [Ulichney 1988; Balzer et al. 2009; Lagae and Dutre 2008; Heck et al. 2013; Öztireli and Gross 2012] with a (close to) zero power spectral density (PSD) in low frequency region and a constant power spectrum in high frequency region. An ideal example of this idea is the *Step blue noise* proposed by Heck et al. [2013] whose spectrum is a step function that is zero below some frequency k_0 and constant anywhere else. Such a sampling pattern perfectly recovers signals with frequencies below k_0 and map all higher frequencies to white noise. Step blue noise samples are also ideal from the perspective of variance in Monte Carlo integration. In [Pilleboue et al. 2015], the authors showed that the flatter the shape of the power spectral density in the low frequency region, the faster the variance converges in numerical integration schemes such as Monte Carlo integration. Thus, the power spectrum must contain a large range of low frequencies for which the spectrum is exactly equal to zero. However, as discussed in detail in [Heck et al. 2013] such "perfect" sampling PSDs are only realizable[1] for a very small k_0 which limits their applicability in practice. To increase the size of the zero region, i.e., k_0, one must give up some of the blue noise characteristics and thus, accept some visible aliasing.

As a solution, Heck et al. introduced *Single Peak blue noise* which adds a mid-frequency peak centered at k_0 to the power spectrum.

[1] A realizable PSD implies that there exists a corresponding point sampling pattern. Every sampling pattern has a corresponding PSD yet the reverse is not necessarily true.

By varying the height and the width of this peak, one can increase the value of k_0 for which the spectrum remains realizable. The downsides are that the spectrum is no longer zero below k_0, which introduces some low frequency artifacts and the peak introduces aliasing in mid-frequency region. Besides the immediate effects on the observed artifacts, another crucial downside is that unlike Step blue noise, the Single Peak spectrum is no longer mathematically tractable, i.e., closed form expressions for the purpose of optimization do not exist. Consequently, optimizing the height, width and k_0 parameters to obtain a realizable spectrum becomes an exhaustive trial and error process. Furthermore, the effects of different parameter choices on the realizability of the spectrum are not known. In particular, there does not exist a clear trade-off between the height and the width of the peak with the latter being especially sensitive. In practice, Heck et al.[2013] suggest to fix a k_0 and width and increase the height (or noise) empirically until a realizable distribution is found. Surprisingly, we find that increasing noise in the power spectra may not always guarantee realizability. The realizability of a blue noise distribution can be verified by ensuring that its corresponding Pair Correlation Function (PCF), $G(r)$, is non-negative for all r. This trial and error approach may fail as spectrum can become unrealizable for larger peaks. This motivates the development of a sound mathematical framework to optimize blue noise sampling patterns.

To address the shortcomings of existing blue noise patterns, we introduce a new family of blue noise called *Stair blue noise*. Unlike Single Peak blue noise, Stair blue noise is mathematically tractable, thereby enabling the designer to $1)$ gain theoretical insights into the sampling pattern and, $2)$ perform parameter optimization to obtain the optimal sampling distribution. Stair blue noise also preserves a perfect zero-region below k_0, thereby providing the user an intuitive means to trade the severity of the artifacts in exchange for the range of frequencies affected. We demonstrate that our approach produces realizable spectra with significantly larger k_0 as well as lower high frequency oscillations than existing blue noise approaches (Figure 1). In order to synthesize blue noise distributions, we adopt an approach similar to [Öztireli and Gross 2012] where the blue noise spectrum is translated into the spatial domain for sample construction. In particular, we propose to employ a weighted, least squares based gradient descent optimization approach coupled with an unbiased PCF estimator to accurately match the target PCF. Image reconstruction results with synthetic functions show that the proposed Stair blue noise distribution leads to improved visual quality in comparison to existing blue noise families.

2 Related Work

In this section, we briefly review some of the prior work on the construction of sampling patterns with blue noise properties.

2.1 Blue Noise Sample Synthesis

Use of irregular sampling patterns is a commonly adopted approach to suppress structured artifacts (e.g. moire artifacts) [Ulichney 1988]. Sampling patterns are typically characterized by their Fourier spectra, and *blue noise* corresponds to the family of distributions with zero energy in the low-frequency region. Poisson disk patterns [Cook 1986; Lagae and Dutre 2008], which are a random arrangement of non-overlapping disks with a predefined radius R, is one of the earliest known distributions with blue noise properties. In particular, its Fourier spectra can be characterized by a peak at the origin, surrounded by a zero-valued low-frequency region, and its remaining energy being smoothly distributed in the high-frequency region. *Dart throwing*-type approaches, which incrementally construct the point set by generating random candidate points that are accepted if their distance to all existing points is at least R, have been used in practice. The performance of dart throwing depends directly on the rejection rate, so the algorithm becomes significantly slower as more and more points are added. Consequently, the authors in [Dunbar and Humphreys 2006; Ebeida et al. 2012; Bridson 2007; Ebeida et al. 2014; Wei 2010] created efficient implementations of the dart throwing algorithm for Poisson disk sampling by maintaining novel data structures to effectively track and sample empty regions. More recently in [Kailkhura et al. 2016], the authors showed that by defining the Poisson disk sampling pattern using the pair correlation function (spatial statistics), one can optimize for parameters (e.g. sample size) that will lead to reduced aliasing in comparison to existing dart throwing techniques. *Iterative relaxation* is another important technique for generating point distributions, which typically starts with an initial point set (e.g. Dart throwing) and optimize the point locations using Lloyd iterations [Lloyd 1982] until convergence. Some popular algorithms based on this approach include capacity constrained Voronoi tessellation (CCVT) [Balzer et al. 2009], and farthest point optimization (FPO) [Schlömer et al. 2011]. An inherent challenge with dart throwing and iterative relaxation approaches is their computational complexity, and hence approximate *tiling* based sample construction methods have been developed [Kopf et al. 2006; Wachtel et al. 2014]. The core idea in these methods is to pre-compute one or more tiles and then place them next to each other to form point sets of arbitrary sizes. Though they are known to produce strong sampling artifacts, they are sometimes preferred in real-time applications.

2.2 Parameterizing Blue Noise Construction

A common challenge with all aforementioned approaches is that the properties of the resulting blue noise spectrum cannot be directly controlled. In other words, the impact of the different parameter choices on the sampling pattern and its realizability is not known. As a first step towards addressing this challenge, Heck et al.[2013], proposed *Step blue noise*, which is characterized by zero energy in the low-frequency region and a flat spectrum in the high frequency region. This parameterization enables a designer to construct an optimal blue noise pattern for a given sample budget. However, the requirement to achieve a flat spectrum in the high frequency region directly trades off with the size of the zero region. This has motivated the design of a relaxed blue noise family, *Single Peak*, which introduced a peak (structured aliasing) in the mid-frequency region to increase the zero region. This relaxation, however, makes the blue noise construction mathematically intractable and consequently, unlike Step blue noise, its analysis is not straightforward. With such parametric approaches, sample synthesis corresponds to choosing samples that match the desired spectral characteristics. In particular, spectrum matching algorithms reformulate this problem into the spatial domain, and directly adjust the relative positioning of points by applying a force to each point [Zhou et al. 2012; Heck et al. 2013]. Alternately, in [Öztireli and Gross 2012], the authors adopt gradient-descent based optimization to match the desired spatial characteristics. However, their algorithm results in a poor-quality matching in the low radius regions, and the use of a biased estimator for measuring the spatial statistics affects the sample quality. Some other approaches for blue noise point synthesis are given in [Jiang et al. 2015; Fattal 2011].

Our contributions in this paper can be summarized as follows:

- We analyze the Single Peak blue noise formulation and empirically show the non-monotonicity of its realizability with respect to all its parameters, i.e., increasing noise in the Single Peak spectra does not always make it realizable;

- We propose *Stair blue noise*, a mathematically tractable generalization of Step blue noise;
- Using Fourier analysis, we identify a subset of *Stair blue noise* distributions that are guaranteed to be realizable and for which we derive theoretical bounds on all the parameters leading to optimal Stair blue noise distributions for a given sample budget;
- Adopting an unbiased PCF estimator [Stoyan et al. 1993], we develop a weighted non-linear least squares optimization approach to accurately match a given target PCF; and
- We demonstrate that Stair blue noise achieves a larger zero region, while producing lesser oscillations in the low-frequency and mid-frequency regions when compared to the Single Peak variant.

3 Background

The discussion below relies on a number of concepts from Fourier analysis and spatial statistics. We briefly review the necessary background and refer the reader to [Illian et al. 2008] for a more in-depth discussion.

3.1 Analysis of Point Distributions

Fourier analysis is a standard approach for understanding the properties of sampling patterns. To assess the quality of sampling distributions, one can analyze their spectral properties such as the power spectral density (PSD). Alternately, the quality of sampling patterns can also be analyzed using spatial statistics, such as, the pair correlation function (PCF) [Öztireli and Gross 2012].

Power Spectral Density: For a finite set of N points, $\{\mathbf{x}_j\}_{j=1}^N$, in a region with unit volume, the radially-averaged power spectral density describes how the signal power is distributed over frequencies. It is formally defined as

$$P(\mathbf{k}) = \frac{1}{N}\sum_{j,\ell} e^{-2\pi i \mathbf{k}.(\mathbf{x}_\ell - \mathbf{x}_j)}, \tag{1}$$

where $\mathbf{k}$ is the vector of frequencies.

Pair Correlation Function: A PCF describes the joint probability of having points at two locations at the same time. A precise definition of the PCF can be given in terms of the intensity λ and product density ρ of a point process [Öztireli and Gross 2012]. The intensity $\lambda(X)$ of a point process X is the average number of points in an infinitesimal volume around X. For isotropic point processes, this is a constant value λ. To define the product density, let $\{B_i\}$ denote the set of infinitesimal spheres around the points, and $\{dV_i\}$ denote the volume measures of B_i. Then, we have $P(\mathbf{x_1}, \cdots, \mathbf{x_N}) = \beta(\mathbf{x_1}, \cdots, \mathbf{x_N}) dV_1 \cdots dV_N$. In the isotropic case, for a pair of points, β depends only on the distance between the points, hence one can write $\beta(\mathbf{x_i}, \mathbf{x_j}) = \beta(||\mathbf{x_i} - \mathbf{x_j}||) = \beta(r)$ and $P(r) = \beta(r)dxdy$. The PCF is then defined as

$$G(r) = \frac{\beta(r)}{\lambda^2}. \tag{2}$$

Relating PSD and PCF: The PSD and the PCF of a point distribution are related via the Fourier transform as follows:

$$\begin{aligned} P(\mathbf{k}) &= 1 + \rho F\left(G(\mathbf{r}) - 1\right) \\ &= 1 + \rho \int_{\mathbb{R}^d} \left(G(\mathbf{r}) - 1\right) \exp(-i\mathbf{k}.\mathbf{r}) d\mathbf{r} \end{aligned}$$

where $\rho = N/V$, with V being volume of the sampling region[2], and $F(.)$ denotes the 2-dimensional Fourier transform. Note that, for radially symmetric or isotropic functions the above relationship simplifies to

$$P(k) = 1 + 2\pi\rho H\left[G(r)\right].$$

In the above equation, $H[.]$ denotes a 1-d Hankel transform, i.e.,

$$H(f(k)) = \int_0^\infty k J_0(kr) f(k) dk.$$

where $J_0(.)$ is the Bessel function of order zero. Note that, the Hankel transform has the following inverse property:

$$H_0^{-1}(f(r)) = \int_0^\infty r J_0(kr) f(r) dr.$$

Using the above property, one can show that

$$G(r) = 1 + \frac{1}{2\pi\rho} H\left[P(k) - 1\right]. \tag{3}$$

Realizability: The two necessary mathematical conditions [3] that a sampling pattern must satisfy to be realizable [Uche et al. 2006] are: (a) its PSD must be non-negative, i.e., $P(k) \geq 0,\ \forall k$, and (b) its pair correlation function must be non-negative, i.e., $G(r) \geq 0,\ \forall r$.

3.2 Blue Noise Distribution

Blue noise distributions are aimed at replacing visible aliasing artifacts with incoherent noise, and its properties are typically defined in the spectral domain. More specifically, a blue noise power spectrum should satisfy the following two requirements: (a) the spectrum should be close to zero in the low frequency region, which indicates the range of frequencies that can be represented with almost no aliasing; (b) the spectrum should be a constant in mid and high frequency regions or contain minimal amount of oscillations in the power spectrum to reduce the risk of aliasing. The low frequency band with minimal energy is referred to as the *zero region*. A variety of blue noise distributions have been considered in the literature [Heck et al. 2013], and they can be classified into two broad categories: (a) low aliasing blue noise (e.g. Step blue noise) that maps the aliasing artifacts to broadband noise, and (b) more flexible blue noise families (e.g. Single Peak blue noise) that guarantee low or zero aliasing in a larger range of low frequencies by introducing oscillations at high frequency region. Note that, the proposed Stair Blue Noise falls into the latter category.

Step blue noise: The power spectrum of Step blue noise is defined as

$$P(k - k_0) = \begin{cases} 0 & \text{if } k \leq k_0, \\ 1 & \text{if } k > k_0. \end{cases} \tag{4}$$

In the above equation, the zero region $0 \leq k \leq k_0$ indicates the range of frequencies that can be represented with no aliasing and the flat region $k > k_0$ guarantees that aliasing artifacts are mapped to broadband noise, which is not visually perceptible.

Single Peak blue noise: The power spectrum of Single Peak blue noise is defined as

$$P(k) = G_{\sigma_g} * \left(P_g \delta(k - k_0) + P(k - k_0)\right), \tag{5}$$

which computes the sum of a Dirac peak of power P_g at frequency k_0 and the step function (also at k_0), followed by convolution with the Gaussian kernel G_{σ_g} (width σ_g).

[2] In this paper, for all our experiments, we consider 1×1 sampling region and, therefore, $V = 1$.

[3] Whether or not these two conditions are not only necessary but also sufficient is still an open question (however, no counterexamples are known).

3.3 Analysis of Single Peak Blue Noise

As discussed above, not all power spectra are realizable. Therefore, given a parameterized family of spectra, i.e. Single Peak blue noise, and a desired number of samples N the goal is to find the "optimal" realizable spectrum. Intuitively, there exist three competing objectives: The first is to maximize the zero region (k_0); the second is to minimize the mid-frequency power peak; and the last is to minimize N. For Single Peak blue noise this roughly corresponds to trading k_0 in exchange for an increase in both P_g and σ_g or an increase in N. Unfortunately, the Hankel transform of the Single Peak spectrum cannot be derived in closed form but can only be approximated numerically. As a result, optimizing for any of the four parameters is an empirical process in which one proposes a certain spectrum and numerically approximates the corresponding PCF to check for realizability. The empirical nature of this approach does not provide any guarantees on optimality and more importantly it provides little insight into the effects of certain parameter choices. In particular, [Heck et al. 2013] propose to first select N and k_0 and then adjust P_g and σ_g ensure realizability.

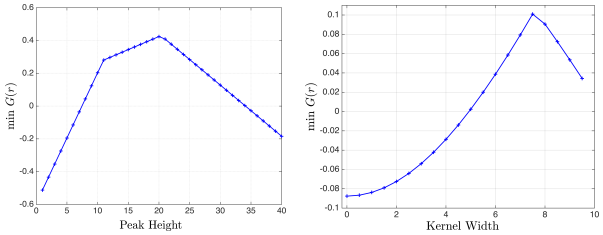

(a) (b)

Figure 2: *Realizability of a Single Peak blue noise spectrum for a given k_0 and N: (a) for varying P_g with $\sigma_g = 1$ and, (b) for varying σ_g with $P_g = 10$. Spectra with $\min\ G(r) \geq 0$ are realizable, however, this property does not change monotonically. Counter-intuitively, increasing either the severity of aliasing or the affected frequency range may make a Single Peak blue noise spectrum unrealizable.*

This approach might suggest that both these parameters affect the PCF monotonically, i.e. increasing P_g or σ_g leads to realizable distributions, and that they can be traded in exchange of one another, i.e. increasing σ_g allows decreasing P_g and vice versa. Unfortunately, this is not the case. Note that, it is sufficient to provide a single counter example to prove that monotonically increasing noise in the Single peak power spectra does not necessarily make it realizable. Unfortunately, the PCF of Single peak blue noise cannot be derived in a closed form. Thus, next we show the counter example numerically.

Figure 2 plots the minimum of the PCF, $\min\ G(r)$, for a given k_0 and N with respect to P_g with a fixed σ_g (a) and a varying σ_g with a fixed P_g (b). Surprisingly, neither curve is monotonic. Therefore, given an unrealizable spectrum, i.e., one with $\min\ G(r) < 0$, it may not be possible to simply increase either parameter to address the problem. Furthermore, this demonstrates that the intuitive trade-off between the height of the frequency peak, i.e., the severity of the aliasing, and its width, i.e., the range of frequencies affected, does not apply in general. This rather unintuitive behavior coupled with the empirical optimization makes the adjustment of the parameters of Single Peak blue noise difficult. Instead, the proposed Stair Blue noise allows closed form solutions for optimizing any of the four parameters, provides theoretical bounds on realizability and preserves the intuitive trade-off between the height and width of the power peak.

4 Proposed Stair Blue Noise

In this section, we define the proposed *Stair* Blue noise distribution, describe its properties and finally derive theoretical bounds for the realizability of the spectrum for all four parameters.

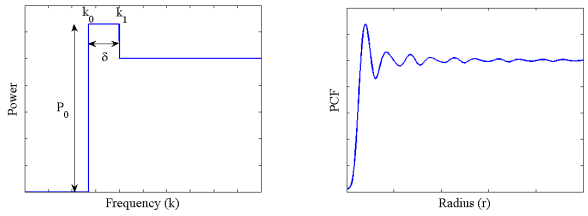

(a) (b)

Figure 3: *Stair Blue Noise: (a) Power Spectral Density. (b) Pair Correlation Function.*

Definition: The Stair Blue noise spectrum P is defined as (see Figure 3(a))

$$P(k) = f(k-k_1) + P_0\left(f(k-k_0) - f(k-k_1)\right), \quad (6)$$

$$\text{with } f(k-k_0) = \left\{ \begin{array}{ll} 0 & \text{if } k \leq k_0 \\ 1 & \text{if } k > k_0 \end{array} \right\},$$

where $k_0 \leq k_1$ and $P_0 \geq 1$.

4.1 Mathematical Tractability

One advantage of Stair blue noise compared to the Single Peak variant is that the PCF for Stair blue noise can be derived in a closed form. Furthermore, for a large class of spectra, including virtually all spectra of practical interest, the realizability constraint can be expressed as a simple inequality. This provides tight bounds on which parameter combinations lead to realizable sampling patterns and new insight on the role that the parameters play on realizability.

Using the Hankel transform as defined in (3), we find:

$$G(r) = 1 - \frac{1}{2\pi\rho}\left[(1-P_0)(k_1)^2\text{Jinc}(rk_1) + P_0(k_0)^2\text{Jinc}(rk_0)\right].$$

The details of this derivation can be found in Appendix A. Figure 3(b) illustrates the PCF corresponding to the Stair blue noise pattern in Figure 3(a). Note, that Step blue noise is a special case with $P_0 = 1$, i.e.,

$$G(r) = 1 - \frac{1}{2\pi\rho}(k_0)^2\text{Jinc}(rk_0). \quad (7)$$

To design an optimal Stair blue noise distribution one needs to balance the trade-off between a large zero region and the mid-frequency oscillations in the PSD, while guaranteeing a realizable spectrum. As discussed above, realizability requires $P(k) \geq 0, \forall k$, which for Stair blue noise is true by construction and $G(r) \geq 0, \forall r$. To guarantee the latter, we need to analyze $\min G(r)$ which is non-trivial in general. However, for a large class of Stair blue noise spectra we find that $\arg\min G(r) = 0$. More specifically, with some simple transformations we find that;

$$G(r) = 1 - \frac{V}{2\pi N}\left[\frac{1-P_0}{P_0}\left(\frac{k_1}{k_0}\right)^2\text{Jinc}(rk_1) + \text{Jinc}(rk_0)\right]P_0k_0^2.$$

Dropping the constants, $\arg\min_r G(r)$ is equal to

$$\arg\min_r\left(\frac{P_0-1}{P_0}\left(\frac{k_1}{k_0}\right)^2\text{Jinc}(rk_1) - \text{Jinc}(rk_0)\right). \quad (8)$$

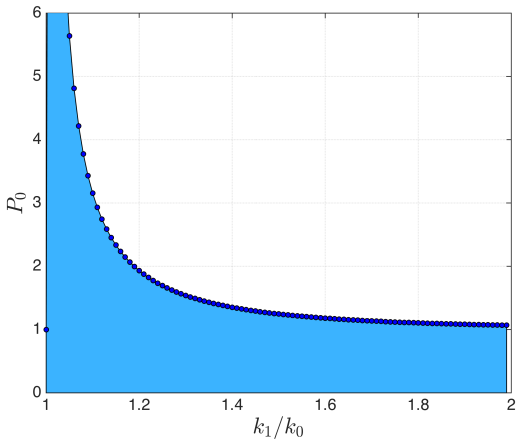

Figure 4: *For tractable analysis, we restrict the Stair blue noise family to the cases with* $\arg\min G(r) = 0$ *(blue area). This restriction includes virtually all blue noise patterns of practical interest.*

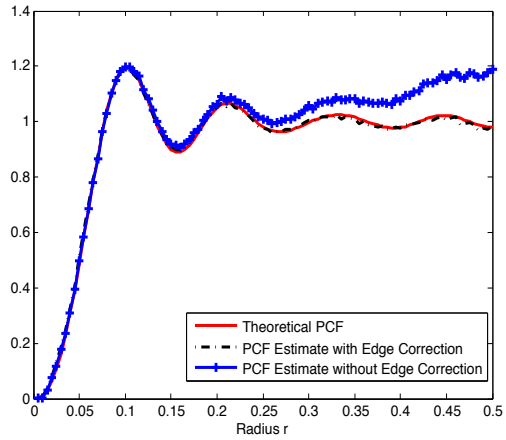

Figure 5: *Kernel Density Estimation of PCF of Stair Blue Noise Sampling Patterns with* $(N = 200, k_0 = 55, P_0 = 1.2, \delta = 20)$.

Setting $A = \frac{P_0-1}{P_0}\left(\frac{k_1}{k_0}\right)^2$, we find that

$$\begin{aligned}
& \arg\min_r G(r) && = && 0 && \\
\Leftrightarrow\quad & A\,\mathrm{Jinc}(0) - \mathrm{Jinc}(0) && \leq && A\,\mathrm{Jinc}(rk_1) - \mathrm{Jinc}(rk_0) && \forall r \\
\Leftrightarrow\quad & A\tfrac{1}{2} - \tfrac{1}{2} && \leq && A\,\mathrm{Jinc}(rk_1) - J(rk_0) && \forall r \\
\Leftrightarrow\quad & A\left(\tfrac{1}{2} - \mathrm{Jinc}(rk_1)\right) && \leq && \tfrac{1}{2} - \mathrm{Jinc}(rk_0) && \forall r \\
\Leftrightarrow\quad & A && \leq && \frac{\frac{1}{2} - \mathrm{Jinc}(rk_0)}{\frac{1}{2} - \mathrm{Jinc}(rk_1)} && \forall r
\end{aligned}$$

Setting $\alpha = k_1/k_0$ and substituting for A this is equivalent to

$$P_0 \leq \frac{\alpha^2}{\alpha^2 - \frac{\frac{1}{2} - \mathrm{Jinc}(rk_0)}{\frac{1}{2} - \mathrm{Jinc}(rk_1)}}. \tag{9}$$

Note that, while difficult to prove analytically, we empirically find that $\frac{\frac{1}{2} - \mathrm{Jinc}(rk_0)}{\frac{1}{2} - \mathrm{Jinc}(rk_0)}$ has its infimum at $r = 0$ and its limit for $r \to 0$ is well defined. Consequently, we can evaluate (9) for all combinations of P_0 and α as shown in Figure 4. The region below the curve indicates spectra with $\arg\min G(r) = 0$ and for the remainder of the paper we consider only this subset of spectra. Note that, this family of Stair blue noise is defined independent of N and the specific values of k_0 and k_1. In particular, this family includes virtually all spectra of practical interest as both large P_0 and large α are likely to cause noticeable artifacts. One immediate observation is that increasing α beyond the Step blue noise case with $\alpha = 1$, realizability is guaranteed for a significantly larger range of α compared to Single Peak blue noise (see Section 6). In practice, we are interested in blue noise distributions which do not have a large mid-frequency peak, and our restricted family produces patterns with a low P_0 even for a reasonably small width $\delta = (k_1 - k_0)$. For example, when $k_0 = 200$ (typically achieved with sample size 4000 in 2D), we can achieve a realizable blue noise distribution with $P_0 = 1.5$ and $k_1 = 280$ ($\alpha = 1.4$). Not only is this width $\delta = 80$ significantly larger than the kernel width that could be used in the Single Peak case but Stair blue noise also causes none of the low frequency artifacts unavoidable in the Single peak spectrum.

The key insight is that for our family of blue noise spectra, the realizability constraint $G(r) \geq 0$ reduces to

$$\min_r G(r) = 1 - \frac{V}{4\pi N}((1-P_0)k_1^2 + P_0 k_0^2) \geq 0, \tag{10}$$

which provides a simple and direct means to optimize the various parameters analytically.

4.2 Optimal Stair Blue Noise

As discussed above, one challenge with the use of Single Peak blue noise is that it is difficult to optimize the spectrum as the exact bounds are not known and the spectrum as a function of the parameters behaves in an unintuitive manner. Instead, (10) provides tight bounds as well as a direct insight into the effects of the various parameters. As expected, increasing N will allow one to realize a spectrum with arbitrary P_0, k_0 and k_1. Furthermore, unlike Single Peak blue noise, the trade-off between the height and width of the mid-frequency peak is monotonic in the sense that any choice of N, P_0 and k_0 will become realizable for a large enough k_1 and conversely any combination of N, k_0 and k_1 for a large enough P_0. More specifically, within our family of Stair blue noise one can derive tight bounds for any of the four parameters as a function of the others:

$$N \geq \frac{V}{4\pi}((1-P_0)k_1^2 + P_0 k_0^2) \tag{11}$$

$$P_0 \geq \frac{4\pi N - V k_1^2}{V(k_0^2 - k_1^2)} \tag{12}$$

$$k_0^2 \leq \frac{4\pi N - V(1-P_0)k_1^2}{V P_0} \tag{13}$$

$$k_1^2 \geq \frac{4\pi N - V P_0 k_0^2}{V(1-P_0)}. \tag{14}$$

Equation (11) highlights the advantages compared to Step blue noise whose required sample budget for a given zero region – $N \geq \frac{V k_0^2}{4\pi}$ – is significantly larger than what can be achieved with even small P_0 and k_1 (note that $P_0 \geq 1$). Furthermore, the effect of increasing k_1 is quadratic compared to the linear one of increasing P_0. This motivates to constrain the peak. This is also interesting in comparison with Single Peak blue noise, which is very sensitive to increases in the width and thus typically requires either higher peaks or smaller zero-regions resulting in more noticeable artifacts for the same sample budget.

5 Synthesis Algorithm

In this section, we describe the proposed approach for synthesizing point sets that match the desired blue noise spectral characteristics.

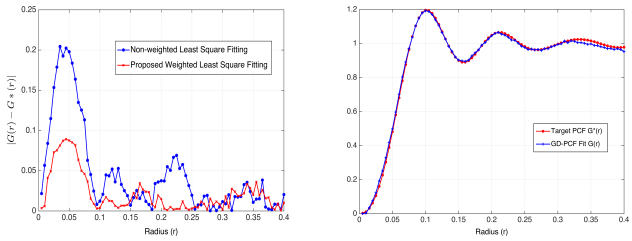

(a) (b)

Figure 6: *Sample synthesis using the proposed PCF matching algorithm. The target PCF is obtained using a Stair blue noise distribution with parameters:* $N = 200, k_0 = 55, P_0 = 1.2, \delta = 20$. *(a) Least squares fitting error with non-weighted and weighted formulations. (b) Estimated PCF of the synthesized samples after* 50 *iterations compared to the target PCF.*

Similar to the approaches in [Öztireli and Gross 2012], we reformulate this problem in the spatial domain by matching the corresponding pair correlation function. Before we present the details of our algorithm, we introduce an unbiased estimator for computing the PCF of a point set.

5.1 PCF Estimation with Edge Correction

Existing approaches for PCF matching employ kernel density estimators to evaluate the PCF of a point set, and these estimators are biased due to the lack of an appropriate edge correction strategy. This bias may arise in calculating PCF due to the fact that sample circles or rings used in calculating point-pattern statistics may fall partially outside the study region and will produce a biased estimate of the PCF unless a correction is applied. Hence, we propose to use an edge corrected, unbiased PCF estimator in our synthesis, originally developed in statistical mathematics [Stoyan et al. 1993].

Let us denote the volume of the sampling region by V_W and its surface area by S_W. When the sampling region is a rectangle with length ℓ and width w, we have $V_W = \ell \times w$ and $S_W = 2(\ell + w)$. Also, let S_E denote the area of the hyper-sphere which is $2\pi r$ in 2-dimensions. In our algorithm, we adopt the following edge corrected kernel density estimator:

$$\hat{G}(r) = \frac{V_W}{\gamma_W} \frac{V_W}{N} \frac{1}{S_E(N-1)} \sum_{i=1}^{N} \sum_{\substack{j=1 \\ i \neq j}}^{N} k\left(r - |x_i - x_j|\right) \quad (15)$$

where $k(.)$ denotes the Gaussian kernel, i.e.,

$$k(z) = \frac{1}{\sqrt{\pi}\sigma} \exp\left(-\frac{z^2}{2\sigma^2}\right), \quad (16)$$

and γ_W is an isotropic set covariance function which can be approximated as

$$\gamma_W = V_W - \frac{S_W}{\pi} r. \quad (17)$$

The term $\frac{V_W}{\gamma_W}$ accounts for edge correction for the unboundedness of the estimator. Figure 5 illustrates the impact of using edge correction in PCF estimation.

5.2 Sample Synthesis using PCF Matching

Our algorithm iteratively transforms an initial random input point set, such that, its PCF matches the target PCF. In particular, we propose a non-linear weighted least squares formulation to optimize for the desired blue noise properties. Let us denote the target PCF by $G^*(r)$. We discretized the radius r into m points $\{r_j\}_{j=1}^{m}$ [4] and minimize the sum of the weighted squares of errors between the target PCF $G^*(r_j)$ and the curve-fit function (kernel density estimator of PCF) $G(r_j)$ over m points. This scalar-valued goodness-of-fit measure is referred to as the chi-squared error criterion and can be posed as a non-linear weighted least squares problem as follows.

$$\arg\min \sum_{j=1}^{M} \left(\frac{G(r_j) - G^*(r_j)}{w_j} \right)^2,$$

where w_j indicates the weight (importance) assigned to the fitting error at radius r_j. This optimization problem can be efficiently solved using a gradient descent algorithm that in our experience converges quickly. In the simplest cases of uniform weights the solution tends to produce a higher fitting error at lower radii r_j (Figure 6(a)). To address this challenge, we use a non-uniform distribution for the weights $\{w_j\}$. These weights are initialized to be uniform and are updated in an adaptive fashion in the gradient descent iterations. The weight w_j at gradient descent iteration $t+1$ is given by:

$$w_j = \frac{1}{|G^t(r_j) - G^*(r_j)|}$$

where $G^t(r_j)$ is the value of the PCF at radius r_j during the gradient descent iteration t.

The weighted non-linear least squares problem is solved iteratively using gradient descent. Starting with a random point set $X = \{x_i\}_{i=1}^{N}$, we iteratively update x_i in the negative gradient direction of the objective function. At each iteration k this can be formally stated as

$$x_i^{k+1} = x_i^k - \lambda \frac{\Delta_i}{|\Delta_i|},$$

where λ is the step size and $\Delta_i = [\Delta_i^1, \Delta_i^2]$ in the normalized gradient is

$$\Delta_i^p = \sum_{i \neq l} \frac{(x_l^p - x_i^p)}{|x_l - x_i|} \sum_{j=1}^{m} \frac{G(r_j)^k - G^*(r_j)}{w_j r_j} \left(|x_l - x_i| - r_j\right) k\left(r_j - |x_i - x_l|\right). \quad (18)$$

We reevaluate the PCF $G(r_j)^k$ of the updated point set after each iteration using the unbiased estimator from the previous section.

While the above algorithm works well in matching realizable, i.e., positive target PSDs/PCFs the results for matching an unrealizable PSD/PCF combination can be unexpected. Given negative values in the target PCF, the algorithm converges to $G(r_j) = 0$ as the best approximation. However, the corresponding PSD may be significantly different from the initial target and can contain significant noise. In practice, it is easy to validate the PCF before starting the synthesis.

In Figure 6, we compare the performance of the proposed weighted least squares based PCF fitting to the unweighted formulation. The target PCF is designed using a stair blue noise sampling pattern with $k_0 = 55, P_0 = 1.2, \delta = 20$, and the PCF matching is carried out with a sampling budget of $N = 200$. The variance of the Gaussian kernel was set at $\sigma^2 = 0.005$ and the step size for the gradient descent algorithm was fixed at 0.001. The initial point set was generated randomly in the region of size (1×1). It can be observed

[4] In this paper, for all the synthesis experiments, we consider r taking values from 0.0001 to 0.4 with a regular sampling with spacing of 0.0001 between samples.

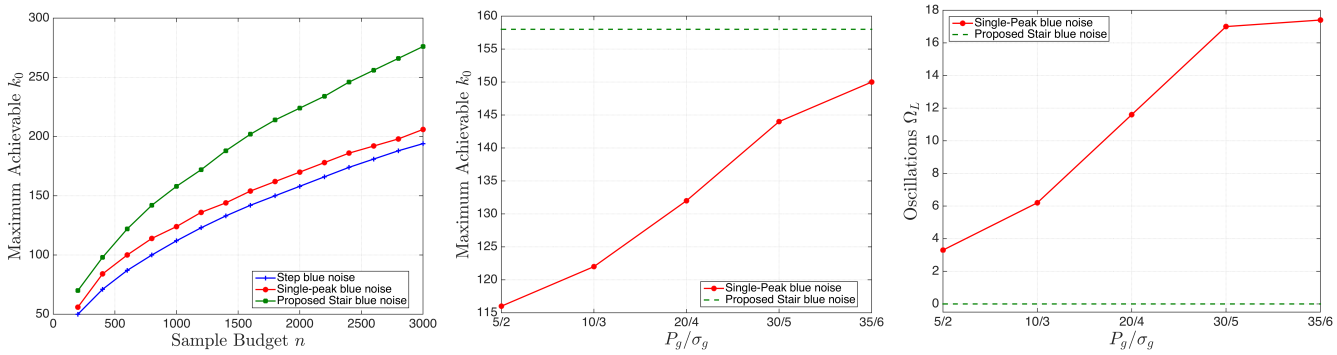

(a) (b) (c)

Figure 7: *Comparison of the maximum achievable k_0 for a given sample budget using different blue noise sampling patterns: (a) Step, Single Peak and Stair blue noise distributions with $P_0 \leq 3$. Impact of the choice of Gaussian peak height (P_g) and width (σ_g) on maximal k_0 (b) and low-frequency oscillations Ω_L (c) for $N = 1000$.*

that the proposed method produces a highly accurate PCF fitting and outperforms the non-weighted case. As expected, the PCF estimation step is a major computational bottleneck in our synthesis algorithm with complexity $O(N^2)$. In practice, one can employ special data structures as given in [Öztireli and Gross 2012] to bring this complexity down to $O(N)$. However, developing strategies to accelerate PCF estimation is not the focus of the work and remains part of our future work.

6 Experimental Results

In this section, we measure the spectral statistics of the proposed Stair blue noise distribution, and present comparisons to Step and Single Peak blue noise constructions. In addition, we use synthetic functions to evaluate the reconstruction quality of synthesized samples in controlling aliasing artifacts.

6.1 Comparison of Spectral Properties

Existing, well-known sampling patterns are aimed at either extending the zero region or reducing structured aliasing. While Step blue noise is optimal in controlling structured aliasing, generalizations such as the Single Peak blue noise and the Stair blue noise can provide a larger zero region at the risk of creating aliasing artifacts at mid frequencies. To assess the quality of the sampling patterns, we analyze their spectral characteristics. Let us define the region from $0 \leq k \leq k_0$ to be low frequency region, the region from $k_0 \leq k \leq k_1$ to be mid frequency region and, the region from $k \geq k_1$ to be high frequency region.

First, we compare the maximum achievable k_0 for Step, Single Peak and Stair blue noise for varying sampling budget assuming $P_0 \leq 3$. Note that, for Single Peak blue noise, k_0 is zero (theoretically) as its power spectrum is non-zero for all k due to the convolution with the infinite support Gaussian kernel. Following [Heck et al. 2013], we instead plot the size of the so called *effective zero region*, k_{eff}, defined as the largest frequency such that average energy in the power spectrum up to this frequency stays below a certain constant. Formally, $k_{eff} = \{\max\ k_0\ : \int_{k=0}^{k_0} P(k)dk \leq \tau\}$. In all our results, we choose τ to be 10^{-3}. The best configuration of Single Peak blue noise is obtained by an exhaustive search over the parameters P_g and σ_g under the constraint $P_0 := \max G(r) \leq 3$. Similarly, the best configuration of Stair blue noise is obtained by optimizing the parameters P_0 and δ under the constraint $P_0 \leq 3$ using results obtained in Section 4.2. Figure 7(a) shows that the Stair blue noise has significantly larger zero region compared to both Step and Single Peak blue noise, without the unavoidable low frequency oscillations of Single Peak blue noise. This result can also be interpreted in the following way: to achieve a certain zero region, the Stair blue noise requires the least number of point samples compared to the Step and Single Peak blue noise. For instance, the zero region achieved by 2000 samples of Step and Single Peak blue noises can be achieved by only 1000 Stair blue noise samples.

Figure 7(b) demonstrates the impact of increasing peak height P_0 of the Single Peak blue noise (by increasing P_g and σ_g as given in (5)) on the maximum achievable k_0. As expected, increasing P_0 results in an increasing zero region for the Single Peak blue noise and for very large values it approaches the maximum achievable k_0 of Stair blue noise.

However, increasing the peak height $P_0 = \max G(r)$ of Single Peak blue noise results in substantial low frequency oscillations. To measure the amount of oscillations, Ω_L, of the power spectrum in the low frequency range, we use the energy in the power spectrum up to a certain frequency (or area under the curve). Formally, it can be represented by

$$\Omega_L = \int_{k=0}^{k_0} P(k)\ dk. \tag{19}$$

For Stair blue noise, Ω_L is zero by construction. However, as shown in Figure 7(c), the Single Peak blue noise introduces significant oscillations in order to approach a zero region k_0 comparable to the Stair blue noise which is likely to cause aliasing. High frequency oscillation performance of all the sampling patterns is the same.

Next, we study the effect of increasing peak height P_0 on the maximum achievable k_0 for the Stair blue noise sampling patterns. Though both the parameters P_0 and δ can be optimized simultaneously to explore all realizable patterns, we consider a more practical setup and fix $\delta = 50$ and vary P_0 between 1 and 3. As shown in Figure 8, the maximal achievable k_0 increases substantially by increasing P_0 especially for large sample sizes at the cost of negligible oscillations.

Figure 9 shows the power spectrum and pair correlation function of a synthesized point set with $N = 1000$ for Step, Single Peak and Stair blue noise distributions. As expected, Stair blue noise has larger zero region compared to both Step and Single Peak blue noises though at the cost of some oscillations at mid frequencies when compared to the Step blue noise.

Figure 10 plots the power spectrum of Stair blue noise for different configurations of P_0 with $N = 1000$. The size of mid frequency

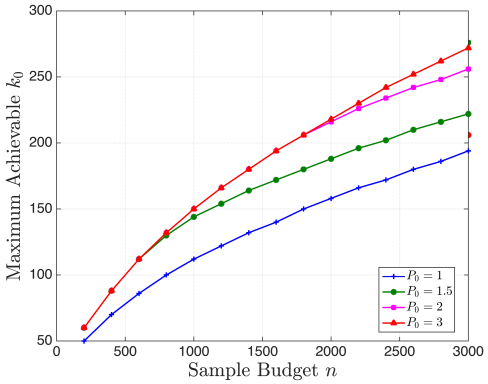

Figure 8: *Maximum achievable k_0 with Stair blue noise for varying P_0 and a fixed $\delta = 50$.*

region δ is optimized to maximize k_0. It can be seen from the figure that the size of zero region increases with the peak height P_0. Depending on the use case the designer can maximize the zero region at the cost of negligible oscillations in the mid frequency range of the power spectrum. For example, the power spectrum of the Stair blue noise with $P_0 = 1.6$ and 1.3 have larger zero region compared to the Step blue noise yet looks similar to power spectrum of Step blue noise (as given in Figure 9) with minimal oscillations.

In Figure 11, we compare the PSD of some common blue noise sampling patterns. The Stair blue noise can achieve similar size zero regions compared to FPO [Schlömer et al. 2011], CCVT [Balzer et al. 2009] and Dart Throwing, however, with significantly less oscillations in mid and high frequencies.

6.2 Reconstruction at Low Sampling Rates

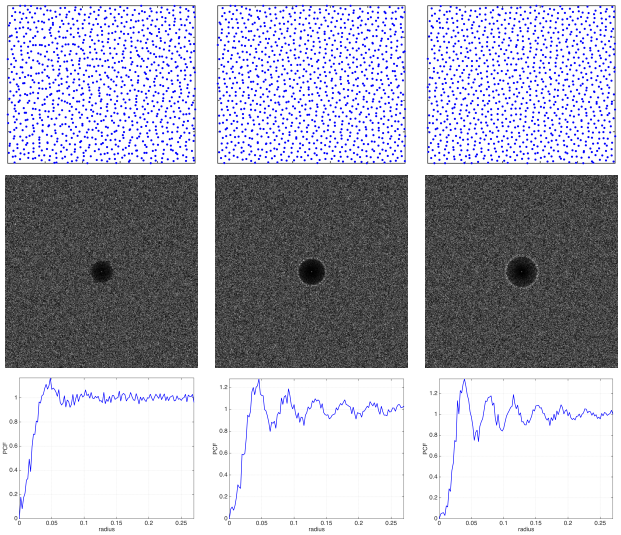

Figure 9: *Synthesized point set, power spectrum and pair correlation function (top-bottom) of Step, Single Peak and Stair blue noise distributions (left-right) for $N = 1000$. The proposed Stair blue noise results in a larger zero region compared to the other two cases*

In this subsection, we focus on undersampling, because the risk of aliasing due to undersampling is the primary reason for using irregular sampling instead of regular sampling. We evaluate the reconstruction performance of different sampling patterns when undersampling. As a test image, we use the common zone plate test function. For undersampling, the zone plate is preferable to more realistic test images since it shows the response for a wide range of frequencies and aliasing effects are not masked by image features. Further, we report the peak signal-to-noise ratio (PSNR) as a quantitative error measure:

$$\text{PSNR} = 20 \ \log_{10} \frac{1}{MSE}$$

where MSE is the mean square error. For all zone plate renderings in this paper, we have tiled toroidal sets of 4096 points over the image-plane and used a Lanczos filter with a support of width 4 for resampling. It can be seen from Figure 12 that Stair blue noise has less noise in the low-frequency region, which typically contains the most salient image information. Images sampled with Single Peak or Step blue noise show a lot more noise in low frequencies. Our method similarly reduces aliasing, but at a significantly lower noise level.

7 Summary and Future Work

To address the shortcomings of existing blue noise patterns this paper introduced a new family of blue noise called *Stair blue noise*. Unlike Single Peak blue noise, Stair blue noise is mathematically tractable, thereby enabling the designer to 1) gain theoretical insights into the sampling pattern and, 2) perform parameter optimization to obtain the optimal sampling distribution. Stair blue noise also preserves a perfect zero-region below k_0, thereby providing the user an intuitive means to trade the severity of the artifacts against the range of frequencies affected. We demonstrated that our approach produces realizable spectra with significantly larger k_0 as well as lesser high frequency oscillations than existing blue noise constructions. Furthermore, we proposed a new algorithm to synthesize point sets given a target spectrum, that produces higher quality blue noise sampling patterns than previous techniques. Proposed Stair blue noise performs better than Step and Single Peak blue noise in image plane sampling tasks. In the future work, we plan to employ data structures to make the proposed synthesis algorithm faster. Another interesting direction of work can be to employ techniques proposed in [Pilleboue et al. 2015] to theoretically analyze the aliasing performance of the Stair blue noise and devise Stair blue noise synthesis algorithm. Further, generation of blue noise samples on manifolds and adaptive sampling can also be investigated.

Acknowledgments

This work was performed under the auspices of the U.S. Department of Energy by Lawrence Livermore National Laboratory under Contract DE-AC52-07NA27344. LLNL-JRNL-703039

References

BALZER, M., SCHLÖMER, T., AND DEUSSEN, O. 2009. Capacity-constrained Point Distributions: A Variant of Lloyd's Method. *ACM Trans. Graph. 28*, 3 (July), 86:1–86:8.

BRIDSON, R. 2007. Fast Poisson Disk Sampling in Arbitrary Dimensions. In *ACM SIGGRAPH 2007 Sketches*, ACM, New York, NY, USA, SIGGRAPH '07.

COOK, R. L. 1986. Stochastic Sampling in Computer Graphics. *ACM Trans. Graph. 5*, 1 (Jan.), 51–72.

DE GOES, F., BREEDEN, K., OSTROMOUKHOV, V., AND DESBRUN, M. 2012. Blue Noise Through Optimal Transport. *ACM Trans. Graph. 31*, 6 (Nov.), 171:1–171:11.

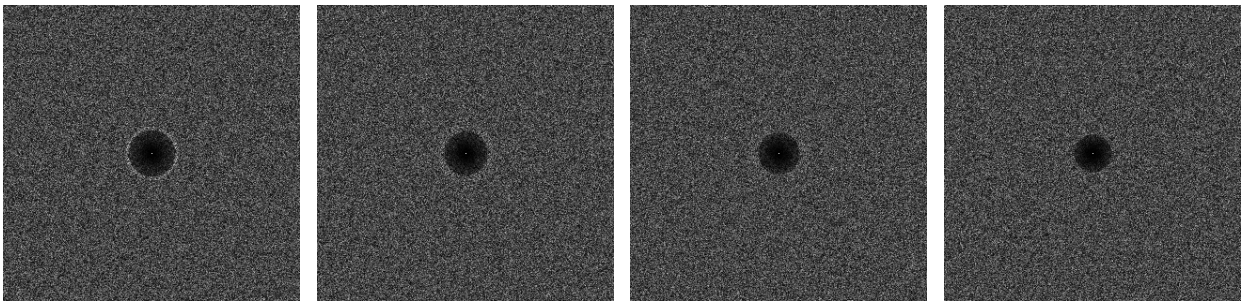

Figure 10: *Stair blue noise with $P_0 = 3, 1.6, 1.3, 1.1$ for $N = 1000$ (left-right).*

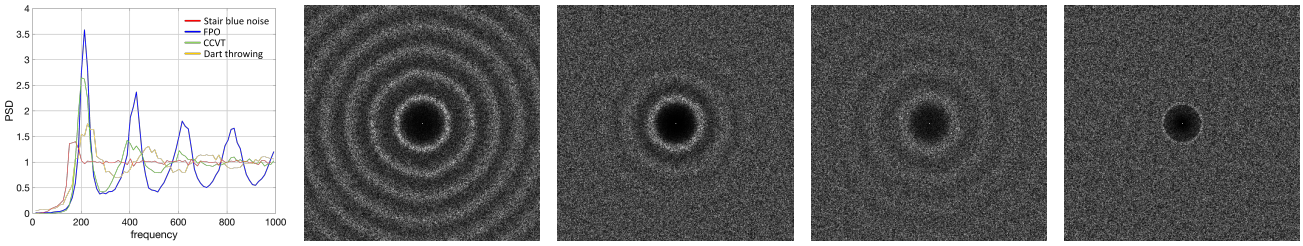

Figure 11: *Comparison of power spectral densities of FPO, CCVT, Dart Throwing and Stair blue noise for $N = 1000$ (left-right).*

DUNBAR, D., AND HUMPHREYS, G. 2006. A Spatial Data Structure for Fast Poisson-disk Sample Generation. *ACM Trans. Graph. 25*, 3 (July), 503–508.

EBEIDA, M. S., DAVIDSON, A. A., PATNEY, A., KNUPP, P. M., MITCHELL, S. A., AND OWENS, J. D. 2011. Efficient Maximal Poisson-disk Sampling. *ACM Trans. Graph. 30*, 4 (July), 49:1–49:12.

EBEIDA, M. S., MITCHELL, S. A., PATNEY, A., DAVIDSON, A. A., AND OWENS, J. D. 2012. A Simple Algorithm for Maximal Poisson-Disk Sampling in High Dimensions. *Computer Graphics Forum 31*, 2pt4, 785–794.

EBEIDA, M. S., PATNEY, A., MITCHELL, S. A., DALBEY, K. R., DAVIDSON, A. A., AND OWENS, J. D. 2014. K-d Darts: Sampling by K-dimensional Flat Searches. *ACM Trans. Graph. 33*, 1 (Feb.), 3:1–3:16.

FATTAL, R. 2011. Blue-noise Point Sampling Using Kernel Density Model. *ACM Trans. Graph. 30*, 4 (July), 48:1–48:12.

GAMITO, M. N., AND MADDOCK, S. C. 2009. Accurate Multidimensional Poisson-disk Sampling. *ACM Trans. Graph. 29*, 1 (Dec.), 8:1–8:19.

HECK, D., SCHLÖMER, T., AND DEUSSEN, O. 2013. Blue Noise Sampling with Controlled Aliasing. *ACM Trans. Graph. 32*, 3 (July), 25:1–25:12.

ILLIAN, J., PENTTINEN, A., STOYAN, H., AND STOYAN, D. 2008. *Statistical Analysis and Modelling of Spatial Point Patterns (Statistics in Practice)*, 1 ed. Wiley-Interscience, Mar.

IP, C. Y., YALÇIN, M. A., LUEBKE, D., AND VARSHNEY, A. 2013. PixelPie: Maximal Poisson-disk Sampling with Rasterization. In *Proceedings of the 5th High-Performance Graphics Conference*, ACM, New York, NY, USA, HPG '13, 17–26.

JIANG, M., ZHOU, Y., WANG, R., SOUTHERN, R., AND ZHANG, J. J. 2015. Blue Noise Sampling Using an SPH-based Method. *ACM Trans. Graph. 34*, 6 (Oct.), 211:1–211:11.

KAILKHURA, B., THIAGARAJAN, J. J., BREMER, P. T., AND VARSHNEY, P. K. 2016. Theoretical guarantees for poisson disk sampling using pair correlation function. In *2016 IEEE International Conference on Acoustics, Speech and Signal Processing (ICASSP)*, 2589–2593.

KOPF, J., COHEN-OR, D., DEUSSEN, O., AND LISCHINSKI, D. 2006. Recursive Wang Tiles for Real-time Blue Noise. *ACM Trans. Graph. 25*, 3 (July), 509–518.

LAGAE, A., AND DUTRE, P. 2008. A Comparison of Methods for Generating Poisson Disk Distributions. *Computer Graphics Forum 27*, 1, 114–129.

LLOYD, S. 1982. Least Squares Quantization in PCM. *IEEE Trans. Inf. Theor. 28*, 2 (Sept.), 129–137.

ÖZTIRELI, A. C., AND GROSS, M. 2012. Analysis and Synthesis of Point Distributions Based on Pair Correlation. *ACM Trans. Graph. 31*, 6 (Nov.), 170:1–170:10.

PILLEBOUE, A., SINGH, G., COEURJOLLY, D., KAZHDAN, M., AND OSTROMOUKHOV, V. 2015. Variance Analysis for Monte Carlo Integration. *ACM Trans. Graph. 34*, 4 (July), 124:1–124:14.

SCHLÖMER, T., HECK, D., AND DEUSSEN, O. 2011. Farthest-point Optimized Point Sets with Maximized Minimum Distance. In *Proceedings of the ACM SIGGRAPH Symposium on High Performance Graphics*, ACM, New York, NY, USA, HPG '11, 135–142.

STOYAN, D., BERTRAM, U., AND WENDROCK, H. 1993. Estimation variances for estimators of product densities and pair correlation functions of planar point processes. *Annals of the Institute of Statistical Mathematics 45*, 2, 211–221.

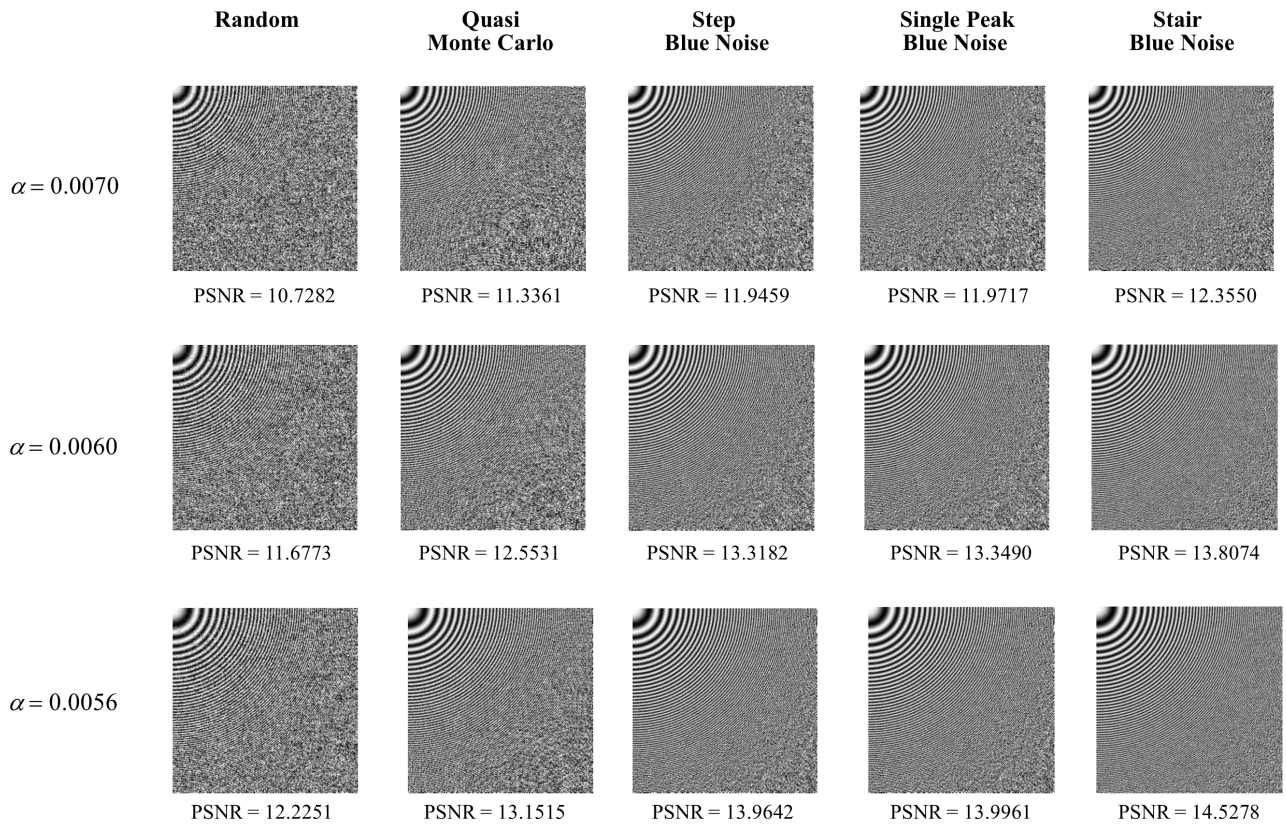

Figure 12: *Reconstruction of the standard zone plate functions $z(r) = (1 + \cos(\alpha r^2))/2$ reveals that the Stair blue noise patterns have superior reconstruction quality. Stair blue noise reduces the aliasing artifacts, and at the same time at a significantly lower noise level (cleaner low frequency content (upper left corner)) and maps all high frequencies (bottom right corner) to white noise.*

UCHE, O., STILLINGER, F., AND TORQUATO, S. 2006. On the realizability of pair correlation functions. *Physica A: Statistical Mechanics and its Applications 360*, 1, 21 – 36.

ULICHNEY, R. A. 1988. Dithering with blue noise. *Proceedings of the IEEE 76*, 1 (Jan), 56–79.

WACHTEL, F., PILLEBOUE, A., COEURJOLLY, D., BREEDEN, K., SINGH, G., CATHELIN, G., DE GOES, F., DESBRUN, M., AND OSTROMOUKHOV, V. 2014. Fast Tile-based Adaptive Sampling with User-specified Fourier Spectra. *ACM Trans. Graph. 33*, 4 (July), 56:1–56:11.

WEI, L.-Y. 2008. Parallel Poisson Disk Sampling. *ACM Trans. Graph. 27*, 3 (Aug.), 20:1–20:9.

WEI, L.-Y. 2010. Multi-class Blue Noise Sampling. *ACM Trans. Graph. 29*, 4 (July), 79:1–79:8.

ZHOU, Y., HUANG, H., WEI, L.-Y., AND WANG, R. 2012. Point Sampling with General Noise Spectrum. *ACM Trans. Graph. 31*, 4 (July), 76:1–76:11.

Appendix

A PCF of Stair Blue Noise

The PCF of the Stair blue noise defined in (6) can be derived using the Hankel transform as follows:

$$
\begin{aligned}
G(r) &= 1 + \frac{1}{2\pi\rho}\left(H\left[(f(k-k_1) + P_0\left(f(k-k_0) - f(k-k_1)\right) - 1)\right]\right) \\
&= 1 + \frac{1}{2\pi\rho}\left(\int_0^\infty kJ_0(kr)[f(k-k_1) \right. \\
&\qquad \left. + P_0\left(f(k-k_0) - f(k-k_1)\right) - 1]dk\right) \\
&= 1 + \frac{1}{2\pi\rho}\left(\int_0^\infty kJ_0(kr)[f(k-k_1) - 1 \right. \\
&\qquad \left. + P_0\left(f(k-k_0) - 1 - (f(k-k_1) - 1)\right)]dk\right) \\
&= 1 - \frac{1}{2\pi\rho}\left((1-P_0)\int_0^{k_1} kJ_0(kr)dk + P_0\int_0^{k_0} kJ_0(kr)dk\right) \\
&= 1 - \frac{1}{2\pi\rho}\left((1-P_0)\frac{k_1}{r}J_1(k_1r) + P_0\frac{k_0}{r}J_1(k_0r)\right) \\
&= 1 - \frac{1}{\rho(2\pi r)}\left[(1-P_0)k_1J_1(k_1r) + P_0k_0J_1(k_0r)\right].
\end{aligned}
$$

Simplifying this expression provides the closed form PCF in (7).